Eur. Phys. J. B **7**, 657–664 (1999)

THE EUROPEAN PHYSICAL JOURNAL B

EDP Sciences

Dynamics of density waves in a two dimensional funnel on an inclined plane

T. Le Pennec, M. Ammi, J.C. Messager, and A. Valance[a]

Groupe Matière Condensée et Matériaux[b], Université de Rennes I, 35042 Rennes Cedex, France

Received: 9 July 1998 / Received in final form and Accepted: 18 September 1998

Abstract. We report here experiments on two-dimensional funnel flow of 1 mm diameter glass beads on an inclined plane. We have investigated the properties of the flow according to the outlet size D of the funnel and the gravity. We have identified three different regimes. For small funnel outlet sizes, there is no significant change in flow density: the flow is rather steady and homogeneous. For intermediate outlet sizes (20 mm $< D <$ 80 mm), the flow is intermittent, consisting of spatially ordered density waves propagating upwards. At bigger outlet sizes, density waves do not exhibit any ordering and the flow dynamics becomes chaotic. In addition, we find that the flow dynamics is independent of the funnel opening angle except close to the channel flow configuration. Finally, it is stressed that the interactions between the beads and the inclined plane play a crucial role in the mechanism of formation of density waves.

PACS. 83.50.v Deformation; material flow – 83.70.Fn Granular solids

1 Introduction

When flowing, granular systems often show fascinating behaviours such as avalanches [1], segregation [2,3], density waves [4–10]... which are mainly due to their dissipative character. In this paper we examine the flow properties of a mono-layer of beads rolling down an inclined plane through a two-dimensional funnel. The interest to use a two-dimensional system lies in the fact that the observation and the measures are direct and non-destructive. This system generates under certain conditions density waves (see Fig. 1) that we want to analyse and understand.

There are many granular systems which exhibit density waves when they are flowing. A first example is given by flows in silos where spatio-temporal variations of density are observed. The density variations are commonly associated with the presence of rupture bands appearing periodically in time at the junction of the cylindrical part and the conical part [11]. These asymmetric bands seem mostly to be the result of arching [12] and dilatancy properties of a dense converging flow. Other types of flows show density waves such as flows in narrow tubes [6,10] or in hour-glass [4,8,13]. In these flows, the density changes are mainly due to the interaction of the grains with the interstitial gas. However, even in absence of gas, flows can exhibit drastic changes of density. In that case, the density variations are traced back to the roughness of the grains [5] which increases the energy dissipation.

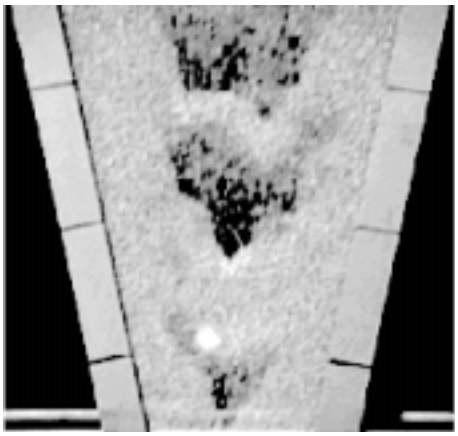

Fig. 1. Snapshot video picture of the flow in the regime where density waves are created. This wave regime appears for large funnel outlet sizes. The snapshot shows only the lower part of the funnel (this corresponds about to 30 cm long). The outlet size is 100 mm and the open angle of the funnel is 24° whereas the inclination angle of the plane is 5.6°.

Flows through two-dimensional funnel on an inclined plane exhibit also density waves, as to be seen below. In this system, the formation of density waves is essentially due to the interactions between the beads and the underlying plane coupled with the geometry of the funnel. Such flows have already been investigated by Veje and Dimon [9]. They have used monodisperse brass beads and examined the flow properties in the case where the funnel is close to a channel geometry (*i.e.*, the funnel angle 2α is smaller than 10°). They have identified three

[a] e-mail: avalance@truffaut.univ-rennes1.fr
[b] UMR 6626

regimes. When $2\alpha > 4°$, the flow is dense and steady (the beads arrange in triangular lattice). An intermittent regime, consisting of quasi-periodic kinematic waves, is found for $0.2° \leq 2\alpha \leq 2°$. Below 0.1° these waves become stationary. In the present study, we are interested in the flow properties in the case where the funnel geometry has a large opening angle (*i.e.*, $2\alpha \sim 60°$). Flows in such a geometry can be compared with discharges in real three-dimensional silos. Furthermore, we have used glass beads whose surface roughness and elastic properties differ from those of brass beads. This difference is revealed to be of paramount importance for the flow behaviour which is very sensitive to the nature of the friction force between the beads and the plane. Contrary to brass beads which tend to arrange in a regular lattice during the flow, glass beads never exhibit such regular arrangement because of their imperfections. As a consequence the flow of glass beads is expected to behave differently. Indeed, in large-angle funnel geometry, flows of brass beads remain homogeneous during the discharge, whereas flows consisting of glass beads have a strong tendency to exhibit density waves. We have analysed the flow properties varying the outlet size of the funnel and the gravity through the inclination angle β of the plane. We have built a phase diagram where three different types of flows have been clearly identified. (i) For small outlet sizes D ($D < 20$ mm) and rather high plane inclination angle β ($4.6° < \beta < 10°$), the flow is found to be nearly homogeneous and steady (regime I). (ii) Either increasing the outlet size or decreasing the plane inclination, one observe a transition towards the formation of density waves. Density waves are created close to the outlet at regular time intervals propagating upwards. As a consequence, the density waves are regularly spaced. This flow regime is commonly called "intermittent flow" (regime II). (iii) Finally, for larger outlet size ($D > 80$ mm) and high gravity ($\beta > 5.6°$), one still observe density waves but their dynamics is no longer regular and looks rather chaotic (regime III).

This paper is organized as follows. In Section 2 we describe our experimental setup. In Section 3 we determine the conditions under which the discharge of the funnel can be initiated, whereas Section 4 is devoted to the analysis of the resulting flow regimes varying the system parameters such as the angle and the outlet size of the funnel, and the inclination of the plane. In Section 5 we focus on the intermittent regime characterized by the presence of periodic density waves and discuss the possible mechanisms of its formation. Finally, in Section 6 we sum up our results and present some outlooks.

2 Experimental setup

Our experimental setup sketched in Figure 2 is composed of an inclined glass plane of 2 m long and 1 m width. The angle β characterises this inclination. The plane is smooth and regularly cleaned after each experiment in order to be sure that no dusts or grease eventually perturb the flow during the measurements. On the plane two PVC bars play the role of a funnel (see Fig. 3). The funnel is filled

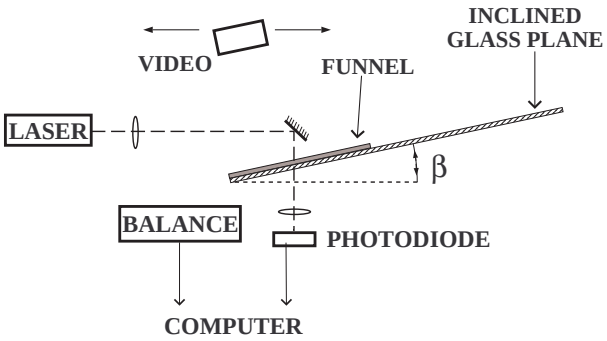

Fig. 2. Experimental setup.

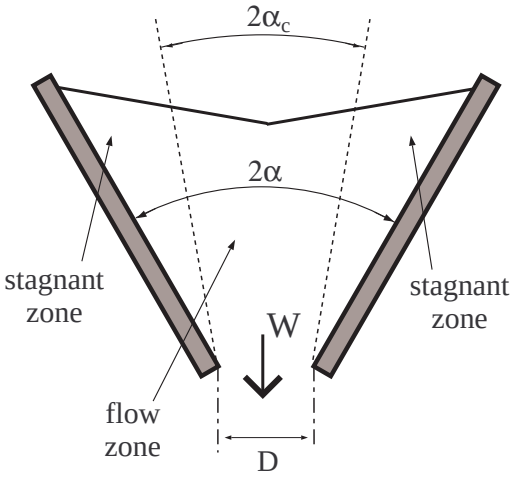

Fig. 3. Schematic view of the funnel.

with a mono-layer of glass beads whose average diameter is $d = 1$ mm and size dispersion is characterized by $\sigma_d \simeq 0.03$ mm. During the discharge, the outflow is measured with a Mettler electronic balance with a sampling frequency of 8 Hz. Moreover the density variations of the flow are measured by optical means. A laser beam is enlarged by lens and deflected on the plane at about 30 cm above the outlet. The quantity of light passing through the plane is then focused on a photo-diode whose signal is amplified and stored with a sampling frequency of 50 Hz. The cross section of the laser beam is about 12 cm^2 which corresponds to the illumination of 1 300 beads for high packing fraction. This optical system allows us to determine the relative flow density. Indeed, the signal received by the photo-diode is intimately related to the flow density. Finally, in order to get an overall view of the flow in the silo, a video camera films the discharge.

3 Initiation of the flow

At a beginning of a run, the outlet is blocked and the funnel is filled with a mono-layer of beads. The inclination of the plane is an important parameter for the flow. The plane should be inclined above a critical angle in order to initiate the flow. In the other hand, the inclination should not be too steep if we want to keep the flow

two-dimensional. The requirement of these two conditions limits the range of our investigation to inclination angles varying from 3° to 10°. The critical plane inclination angle β_c above which the flow can be initiated depends strongly on the initial packing fraction of the pile. Indeed we have found that for a packing fraction $C \approx 0.78$ (loose packing), $\beta_c \approx 2°$. For higher initial packing fraction $C \approx 0.84$ (dense packing) — obtained by tapping slightly on the plane —, β_c goes up to 5°. By increasing the packing fraction, contacts between beads become stronger and one thus has to enhance the gravity force in order to make the pile flow.

As the outlet is unblocked, after a transient period the flow reaches a "permanent" regime which is independent of the initial configuration of the pile. For the runs reported in this paper we have always used a loose packing initial configuration. In that case, the transient is shorter and consequently the "permanent" regime lasts longer.

Although the transient period is not the central point of our preoccupation, we shall make a few comments about its characteristics. The transient is characterised by the propagation of a decompaction front. Immediately after the outlet is unlocked, one can clearly see a front moving upwards. Above the front, the material is compact and the grains are immobile. The rotation of the beads are frustrated by their neighbours and they can not roll as long as the neighbours downhill have not moved. Below the front, the material is dilute and the beads freely fall towards the outlet. The time lag between the motion of the first rows of beads of the pile and the ones at the top is of order of several seconds. The transient is of course sensitive to the initial configuration of the pile.We have noted that the propagation speed V_d of the decompaction front increases as the packing fraction decreases. For $\beta = 5°$, V_d is found to approach 25 $\mathrm{cm\,s^{-1}}$ when the initial packing is loose whereas V_d is of order of 8 $\mathrm{cm\,s^{-1}}$ for dense packing.

The mechanisms of the front propagation is not clearly understood at this moment. We think however that the friction between the beads and thus the surface properties of the beads should play a preponderant role in the decompaction process. We can easily understand that the presence of micro-asperities on bead surface strengthen the contact between beads and increases resistance to rotation. But in the present state of our knowledge we are unable to relate the time needed for a bead to leave the pile to its surface properties nor to the configuration of the pile.

4 General behaviour of the flow

The general features of the flow are sketched in Figure 3. When the funnel angle is rather large (*i.e.*, $2\alpha = 60°$), two types of zones can be distinguished: (i) a stagnant zone and (ii) a flow zone. In the stagnant zone the beads are nearly at rest. The boundary between the two zones is identified as the shear band. The shear bands describe a cone with an opening angle $2\alpha_c \simeq 20°$ (called the angle of approach) that is found to be independent of the opening angle 2α and the outlet size D of the funnel. The mass transfer from the stagnant to the flow zone is mainly produced by avalanches at the free top surface. This type of configuration flow is commonly called *funnel flow*. When the funnel opening angle 2α is lower than the angle of approach $2\alpha_c$, all the beads participate to the flow and the configuration is called *mass flow*.

We have investigated the flow properties according to the outlet size D and the plane inclination β. In the first set of experiments presented in this section, the funnel opening angle has been kept constant and equal to $2\alpha = 60°$. We have distinguished three different regimes whose features are clearly identified thanks to the optical measurements.

When $D < 20$ mm and $4.6° \leq \beta \leq 10°$, the flow looks rather homogeneous and presents no apparent density variations (regime I). The intensity I of the measured optical signal shown in Figure 4a exhibits no significant fluctuations. Furthermore the autocorrelation function $C(\tau)$ [which is defined by $C(\tau) = (\langle I(t)I(t+\tau)\rangle - \langle I\rangle^2)/(\langle I^2\rangle - \langle I\rangle^2)$] does not show any sign of periodicity.

The regime II is characterised by the presence of density waves which are emitted periodically in time from the funnel outlet. This regime is referred to as the intermittent regime. The analysis of our experimental data has lead us to divide this regime into two distinct sub-regimes (IIa and IIb).

The first one (IIa) is characterised by the optical signal shown in Figure 4b. Although the signal does not look very regular, it exhibits peaks that appear nearly periodically in time. Indeed the time correlation function shows a peak at $\tau \simeq 0.5$ indicating the periodicity of the signal. The direct observation of the flow allows us to state that the intensity variation of the optical signal corresponds to the passage of density waves. These waves are created periodically in time with the period T in the vicinity of the funnel outlet and move upwards to the free surface. The optical signal shows moreover that the magnitudes of the density waves in this regime are rather weak and uncorrelated, and undergo large fluctuations. This regime is found to appear for $D < 20$ mm and $3.6 \leq \beta \leq 4.1°$.

The other intermittent regime (IIb) (see Fig 4c) is characterized by a very regular optical signal with a well-defined period T (of order of half a second for the example shown in the figure). This indicates that the density waves are not only emitted regularly in time but they have also the same magnitude. As a consequence, they propagate at the same speed V (of order of 25 cm/s for the example shown in the figure) and exhibit therefore a spatial ordering characterized with a wavelength $\lambda = V_0/T \simeq 12.5$ cm. This regime takes place for larger funnel outlet sizes (20 mm $\leq D <$ 80 mm).

The regime III, although it is also characterized by the presence of density waves, is quite different from the intermittent regime. In this regime, the density waves do not appear regularly in time but are created at erratic time intervals. Furthermore some density waves die out before reaching the free top surface. As a consequence, dynamics of density waves does not exhibit any temporal or spatial

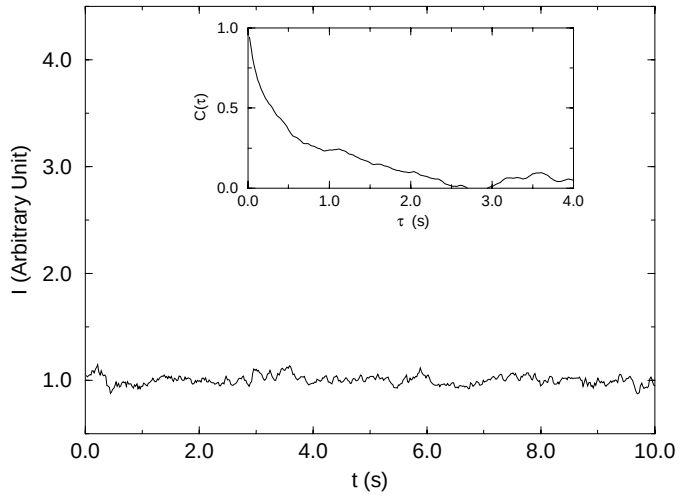

(a)

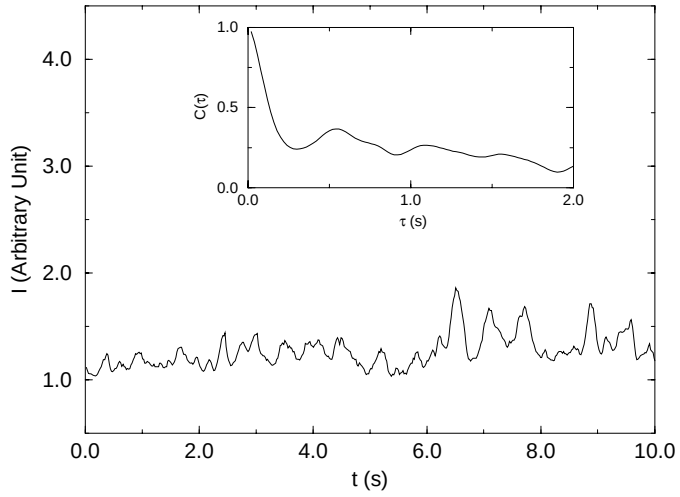

(b)

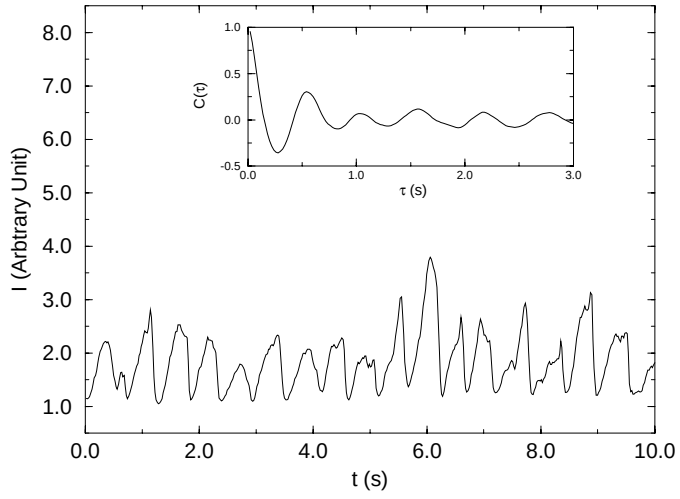

(c)

Fig. 4. Variation of the optical signal during a discharge: (a) regime I [$D = 9$ mm, $\beta = 7°$, $2\alpha = 60°$], (b) regime IIa [$D = 9$ mm, $\beta = 3.6°$, $2\alpha = 60°$], (c) regime IIb [$D = 40$ mm, $\beta = 3.6°$, $2\alpha = 60°$].

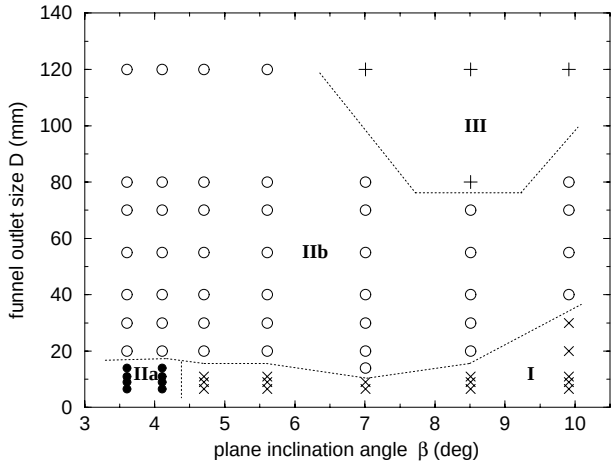

Fig. 5. Phase diagram in the plane (β,D) for a funnel opening angle $2\alpha = 60°$.

ordering and looks rather chaotic. The characterization of this regime is therefore delicate. This chaotic regime is observed for large values of D and β ($D > 80$ mm and $\beta > 5.6°$).

The classification that we have made thanks to the optical measurements allows us to build a phase diagram which is presented in Figure 5. The domains associated to the different regimes are relatively well separated. The transitions from regime IIa to regime IIb, and from regime I to regime IIb which occur by varying the outlet size D are relatively sharp and well defined. This is not the case for the transition from regime IIb to regime III whose location suffers from uncertainties. Indeed, for flows with large outlet sizes ($D \sim 80$ mm), the experimental data are poorly reproducible. This traces back to the fact that at high flow rate the electrostatic forces become important and their magnitude are extremely sensitive to the degree of humidity in the air which must be controlled properly.

5 The intermittent regime

5.1 Experimental results

In order to better understand the mechanisms of formation of the density waves, we focus our attention on the intermittent regime and especially on the regime IIb which exhibits regular density waves. As the optical signal in this regime is quasi-periodic, we define an additional quantity $F_c = \left(\langle I^2\rangle - \langle I\rangle^2\right)^{1/2}/\langle I\rangle$ that will be referred to as the contrast factor (we recall that I is the intensity of the optical signal). This quantity measures the variance of the optical signal normalized by its mean value. (The normalization is needed in order to suppress the effect of the amplification of the measured optical signal.) Physically, F_c is a measure of the magnitude of the density waves observed during a discharge. To be more specific, F_c can be estimated as a function of the minimum and maximum packing fraction of the flow: $F_c \simeq (C_{max} - C_{min})/(C_{max} + C_{min})$. An increase of the

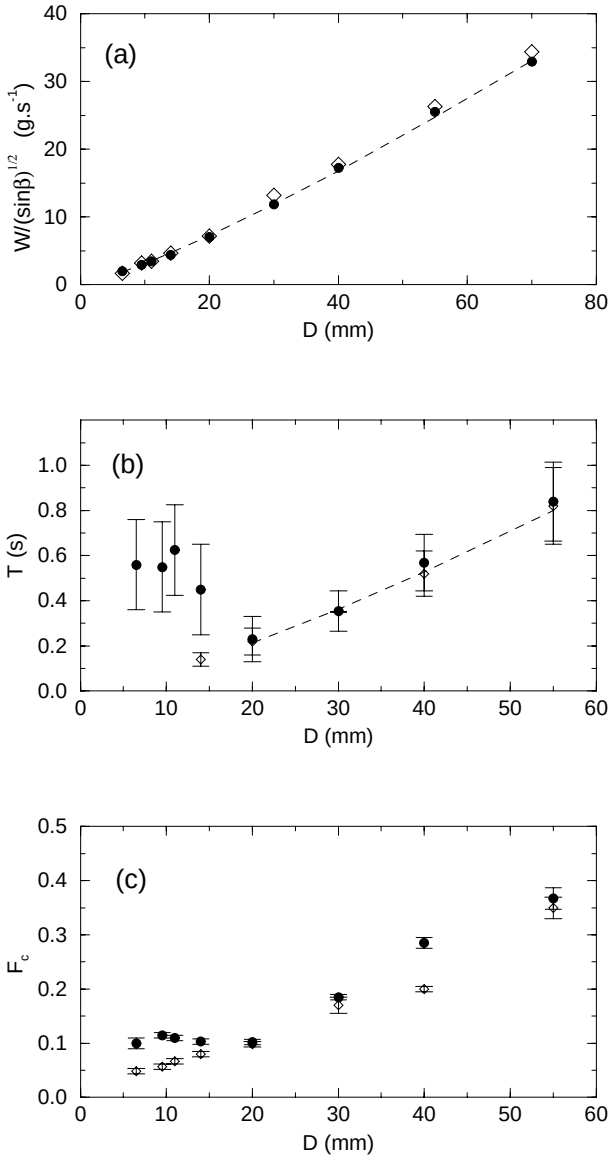

Fig. 6. Variations of the flow rate W (a), the period T (b) and the contrast factor F_c (c) as a function of the outlet size D for two plane inclination angles: $\beta = 3.6°$ (•) and $\beta = 7°$ (⋄). $2\alpha = 60°$.

ratio C_{max}/C_{min} entails a raise of F_c. For a well marked wave (*i.e.*, C_{min} close to 0), F_c tends to 1.

Figure 6 shows the variations of the flow rate W, the period T and the contrast factor F_c as a function of D ranging from 6 to 60 mm. We have displayed the results for two values of the plane inclination angle ($\beta = 3.6°$ (•) and $\beta = 7°$ (⋄)). We can see that the flow rate W increases with the outlet size D. One can also note that when the flow is normalized by $(\sin\beta)^{1/2}$, the two curves corresponding to $\beta = 3.6°$ and $\beta = 7°$ collapse. Thus W seems to scale as $(\sin\beta)^{1/2}$. A further analysis shows in addition that $W \sim D^{1.2}$. A simple dimensional analysis gives $W \sim (g\sin\beta)^{0.5}D^{1.5}$ for a two-dimensional flow (this scaling is in fact known under the name of "Berveloo correlation" [14–16]). The scaling with D is thus slightly different from that given by the Beverloo correlation. Although the difference is relatively tiny, it is tempting to conjecture that this is a signature for the presence of density waves as it is suggested in [16].

The period T and the contrast F_c exhibit different features for the two plan inclinations:

(i) For $\beta = 3.6°$, we can clearly note two different behaviours. When $D < 20$ mm, T and F_c do not vary significantly, whereas for $D > 20$ mm they increase practically linearly with D. This change of behaviour corresponds in fact to the transition from the regime IIa to the regime IIb. The values of the contrast factor F_c ($F_c \simeq 0.1$ which corresponds to a ratio $C_{max}/C_{min} \simeq 1.2$) confirm that the density waves in the regime IIa have a rather weak magnitude. Furthermore their magnitude seems to be independent of the outlet size. In the regime IIb, the magnitude of the density waves get bigger and bigger as the outlet size increases (for $D = 55$ mm, $F_c \simeq 0.36$ which corresponds to a ratio $C_{max}/C_{min} \simeq 2$). We should point out that the contrast factor F_c (or equivalently the wave magnitude) seems to vary continuously at the transition. This is not the case if we look at the period T. One can observe an abrupt decrease of T at the transition which should indicate a change in the mechanism of creation of the density waves.

(ii) For $\beta = 7°$, T and F_c show no transition simply because for such plane inclination the regime IIa does not exist. For $D < 20$ mm the flow is homogeneous (regime I) and there are not any density waves (the contrast factor is nearly zero as can be seen in Fig. 6c). We can note also that for $D > 20$ mm the values of T and F_c coincide with those found for $\beta = 3.6°$. This means that in the regime IIb the period and magnitude of the density waves seems to be insensitive to the plane inclination. Finally, a careful inspection of the data tends to show that $T \sim D$ in the regime IIb.

An other important quantity which is necessary to complete the description of the flow dynamics is the propagation speed of the density waves. We have measured the mean velocity V of the waves as a function of the outlet size D for different gravities (*i.e.*, plane inclination) (see Fig. 7). One can clearly see that the wave velocity decreases with D and increases with the gravity. However, it should be noted that for the inclination $\beta = 3.6°$, two regimes are observed: for $D < 30$ mm (*i.e.*, in the regime IIa), the wave speed remains approximatively constant, whereas for $D > 30$ mm (*i.e.*, in the regime IIb), it decreases. This transition is not seen at higher gravity since only the regime IIb exists. These results confirm that the waves in the regime IIa are of different nature of those of the regime IIb.

The decrease of the wave velocity with the outlet D can be understood thanks to the measurements of the contrast F_c. Indeed, assuming the observed waves are shock waves, we can estimate the propagation speed V of the waves: $V = (C_2V_2 - C_1V_1)/(C_2 - C_1)$ where $C_{1,2}$ and $V_{1,2}$ are the packing fraction and the velocity just before and just after the wave front. C_1 corresponds therefore to the packing fraction C_{max} of the high-density region and C_2 to that of the low-density region (*i.e.*, C_{min}).

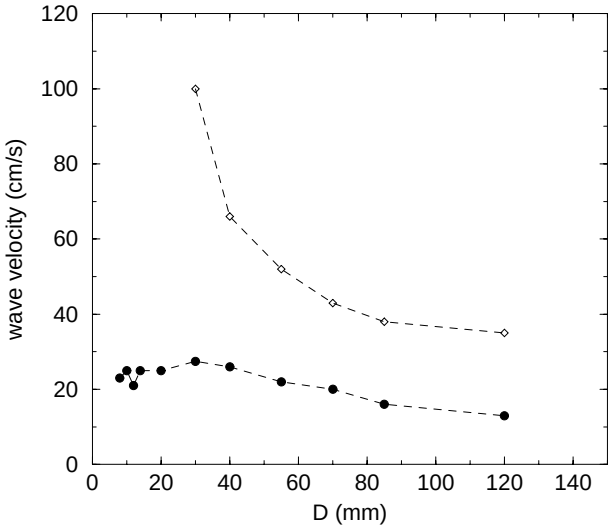

Fig. 7. Average propagation velocity of the density waves as a function of the outlet size for the inclination angles $\beta = 3.6°$ (•) and $\beta = 7°$ (◇). $2\alpha = 60°$.

In addition, since the beads are observed to be momentarily stop at the wave front, we will assume that $V_1 \simeq 0$. V_2 is the velocity V_b of the beads in the low-density region. It follows that the wave velocity is approximatively given by $V = -V_b/(C_{max}/C_{min} - 1)$ (the minus sign indicates that the wave moves in the direction opposite the flow). At high gravity, we find using the data of F_c that the diminution of the wave velocity with the outlet size D can be attributed essentially to the increase of the contrast F_c (which is closely related to C_{max}/C_{min}) (see Fig. 6c) while V_b remains approximatively constant. For $\beta = 7°$, V_b can be estimated at 100 cm/s. At lower gravity (*i.e.*, $\beta = 3.6°$), the behaviour seems to be more complicated since V_b is found to increase significantly with D.

Finally, we have investigated the change in the flow dynamics as we vary the opening angle of the funnel. In Figure 8 are displayed the variation of W, T and F_c as a function of the funnel angle 2α. Unexpectedly, the flow rate has a maximum at $2\alpha \sim 8°$. When one starts from the channel geometry ($2\alpha = 0$) and increases the funnel open angle up to $2\alpha = 8°$, the flow rate increases rapidly. At $2\alpha = 8°$, it reaches a maximum and beyond this value, it decreases regularly. We find that $W \sim \alpha^{-0.1}$ which is quite different from the usual power-law behavior ($W \sim \alpha^{-0.5}$; see [15]). This discrepancy may be again due to the presence of density waves during the discharge. The variations T and F_c as a function of the funnel opening angle show a quite different behaviour. As long as 2α is bigger than 20°, T and F_c remain approximatively constant and as soon as the funnel opening angle gets smaller than 20°, they increase strongly. In particular, T is found to scale as $T \sim \alpha^{-1} \sim (\tan\alpha)^{-1}$. The angle of 20° corresponds exactly to the angle of approach at which the transition between the funnel flow and the mass flow occurs. It seems rather clear that in the funnel flow regime the flow dynamics should be independent of the funnel

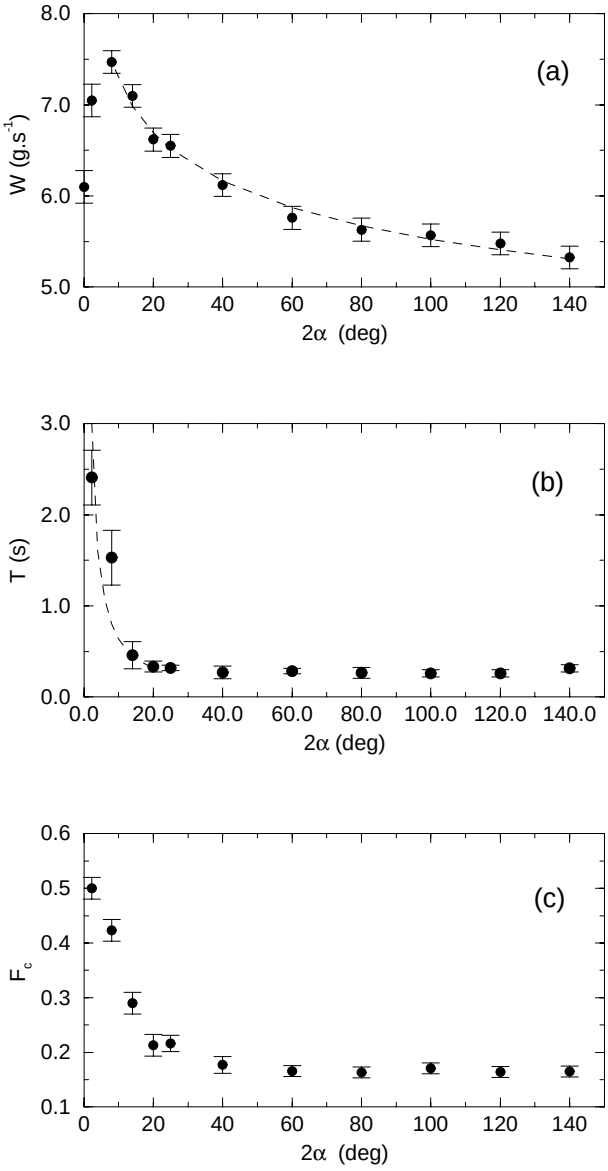

Fig. 8. Variations of the flow rate (a), the period T (b) and the contrast factor F_c (c) as a function of the funnel opening angle 2α. $\beta = 5.6°$ and $D = 45$ mm.

opening angle 2α since the flow is confined in a cone whose effective opening angle is independent of α. Conversely, in the mass flow regime, the flowing region extends over the all funnel and the properties of the density waves are expected to be sensitive to the funnel angle. These features are clearly seen through the behaviours of T and F_c but not through that of W which is quite surprising. First, W is not independent of the opening angle for $2\alpha > 20°$, as we would have expected, and second the presence of a maximum at $2\alpha \sim 8°$ remains unexplained. The first feature can be traced back to the fact that the shear bands close to the funnel outlet are curved. It means that the actual angle of approach measured near the outlet is larger than $2\alpha \simeq 20°$. Furthermore it increases with the funnel open angle. Thus, since the flow rate will depend on the angle of approach at the outlet, this may explain why

beyond $2\alpha \simeq 20^\circ$ the flow rate decreases[1]. The second feature (*i.e.*, the maximum in the flow rate) has already been observed by Veje and Dimon [9] in their experiment using brass beads. However, whereas in their experiment the maximum in the flow rate is clearly a consequence of the fact that the funnel was bed from a reservoir, in our experiment where there is no reservoir (the funnel is just filled up to a certain level) this occurs for completely different reasons which have not been yet identified.

5.2 Interpretation

Here we will focus our attention on the formation mechanism of the density waves observed in the regime II and will propose explanations to interpret some of our experimental results.

We have seen that the frequency (or the period T) of the creation of density waves is essentially controlled by the geometry properties of the funnel. Indeed, T scales as $T \sim D/\tan\theta$ where D is the outlet size of the funnel and θ the opening angle of the flowing region. We propose a simple model which allows us to qualitatively explain the behaviour of the period T.

First of all, we should recall that the density waves are created close to the outlet of the funnel and propagate upwards to the free surface. A density wave can be seen as a plug (*i.e.* a high density region) that is formed at the funnel outlet and then moves upwards. The plug is fed by the material coming from above while below the plug the material is dilute and falls nearly freely. As the plug moves upwards, more and more material is leaving the plug simply because the lateral extent of the plug gets larger. Furthermore, the falling material, due to the funnel geometry, gets more and more compactified as it approaches the outlet. As a consequence, we expect that the flow at the orifice will block again; a new plug is then formed at the outlet and a new cycle starts.

On the grounds of this mechanism we are able to estimate the frequency (or the period T) of apparition of plugs at the outlet. We will note, as previously, C_{max} the packing fraction of the plugs. We will assume that a plug is created at the outlet as soon as the packing fraction close to the orifice reaches C_{max}.

Let us imagine that a plug has been created and moves upwards with a velocity V. We want to estimate the packing fraction of the flow at the outlet as the plug moves upwards. The amount of material per unit time leaving the plug is proportional to $C_{max} l|V|$ where l is the lateral extent of the plug. It should be noted that the lateral extent l depends on the distance z (or the height) between the orifice and the plug; l is simply related to z by $z = (l - D)/(2\tan\theta)$ where 2θ is the opening angle of the cone defining the flowing region (*i.e.*, $\theta = \alpha$ for $\alpha < \alpha_c$ and $\theta = \alpha_c$ for $\alpha > \alpha_c$). In virtue of mass conservation, we can state that the material, which detached from the plug at the height z, arrives at the outlet with a packing fraction C given by $C = C_{max} l|V|/[D(|V| + |V_b|)]$ (V_b is the velocity of the beads in the flowing region to be assumed uniform in a first approximation). The flow will stop as soon as C reaches C_{max} and thus a new plug will appear. This happens when the material arriving at the outlet is that which detached from the plug when the latter was at a critical height z_c corresponding to a lateral size l_c given by $l_c = D(1 + |V_b/V|)$. The critical height is then easily found to be $z_c = D(|V_b/V|)/(2\tan\theta)$. As a consequence, the elapsed time T between the formation of two successive plugs is given by $T = z_c/|V| + z_c/|V_b|$ (*i.e.*, the time needed by the plug to reach the height z_c plus the time corresponding to the fall of the beads). This yields

$$T \simeq A\frac{D}{2\tan\theta} \tag{1}$$

where

$$A = \frac{|V_b|}{|V|}\left(\frac{1}{|V|} + \frac{1}{|V_b|}\right). \tag{2}$$

We thus recover the geometrical factor $D/\tan\theta$ in the expression of T. In the light of the experimental results, we can state that the evolution of T with the outlet size and the opening angle of the funnel is dominated by this geometrical factor. We should, however, point out that A is not constant; it varies with D and θ in a complicated manner, but its variation brings only a small correction to the major evolution of T given by the geometrical factor.

In addition the model suggests that when the funnel is close to a channel geometry the period goes to infinity. This means that the density waves should disappear. This is not what experiment shows: in a channel geometry density waves are still present and are emitted periodically in time with a finite period. We can thus conclude that our model, which is essentially based on geometrical arguments, is not suitable for channel geometry where the mechanism of formation of density waves should be rather sought in the dynamical properties of the flow.

The relative success of the model shows that the geometry plays a crucial role in the formation of density waves in a funnel. Of course, our model is very crude and a further analysis taking into account the dynamical aspects of the problem and the interactions between the beads and the plane would be strongly desired in order to have a deeper understanding of the formation of density waves.

6 Conclusion

We have reported experiments on two-dimensional funnel flow of 1 mm diameter glass beads on an inclined plane and focused our attention on the flow properties as a function of the funnel outlet size, the opening angle, and the gravity. We have found that in large-angle funnel geometry (*i.e.*, in the funnel flow configuration) the flow dynamics is essentially determined by the outlet size D of the funnel. For $D < 20$ mm, the flow density remains steady and homogeneous while for intermediate outlet sizes, the flow is intermittent consisting of spatially ordered density waves propagations upwards. Finally for bigger outlet

[1] This explanation has been suggested by the referee

sizes ($D > 80$ mm), density fluctuations become chaotic. In the intermittent regime, the density waves are generated periodically in time with a period T which is proportional to D and is independent of the funnel opening angle (as soon as the flow is of funnel type). The flow rate W increases with the gravity and the outlet size D ($W \sim (g \sin\beta)^{0.5} D^{1.2}$). The scaling with D differs slightly from the Beverloo correlation ($W \sim g^{0.5} D^{1.5}$) and may be a signature of the presence of density waves. In addition, W is the only measured quantity that varies with the funnel opening angle (even in the funnel flow configuration) which remains unclear. In small-angle funnel geometry (*i.e.*, in the mass flow regime), the flowing zone extends over the whole funnel and therefore the flow rate W and the period T characterizing density wave formation are extremely sensitive to the funnel angle. Furthermore we have seen that the channel is a singular limit of the funnel geometry. The origin of the formation of the density waves should be radically different in both geometries.

Finally we have presented a simple model based on geometrical arguments which allows us to explain qualitatively the variation of the period T as a function of the outlet size and the opening angle of the funnel. However, we are not able to predict the propagation speed of the density waves, as well as the velocity of the beads in the flowing region. To do this, it is absolutely necessary to take into account the dynamical aspects of the problem and the mechanical properties of granular media. We think that the dissipation due to friction between the beads and the plane plays a crucial role in the formation of density waves. A highly dissipative flow favours the formation of density waves.

To gain a deeper understanding of the flow dynamics, it would then be strongly needed to investigate the flow at the grain level, that is to measure the density and velocity field of the flow in the low-density region as a function of the system parameters and the dissipative properties of the beads.

We gratefully acknowledge fruitful discussions with L. Oger and R. Delannay.

References

1. P. Bak, C. Tang, K. Wiesenfeld, Phys. Rev. Lett. **59**, 381 (1987).
2. A. Rosato, K.J. Strandburg, F. Printz, R.H. Swendsen, Phys. Rev. Lett. **58**, 1038 (1987).
3. F. Cantelaube, D. Bideau, Europhys. Lett. **30**, 133 (1995).
4. K.L. Schick, A.A. Verveen, Nature **251**, 599 (1974).
5. G.W. Baxter, B.P. Berhinger, T. Fagaert, R.H. Swendsen, Phys. Rev. Lett. **62**, 2825 (1989).
6. T. Pöchel, J. Phys. I France **4**, 499 (1994).
7. H.J. Herrmann, E. Flekkøy, K. Nagel, G. Peng, G. Ristow, *Traffic and Granular Flow*, edited by D.E. Wolf, M. Schreckenberg, A. Bachem (1993).
8. T. Le Pennec, K.J. Måløy, A. Hansen, M. Ammi, D. Bideau, X.-L. Wu, Phys. Rev. E **53**, 2257 (1996).
9. C.T. Veje, P. Dimon, Phys. Rev. E **54**, 4329 (1996).
10. T. Raafat, J.P. Hulin, H.J. Hermann, Phys. Rev. E **53**, 4345 (1996).
11. J. Lee, S.C. Cowin, J.S. Templeton, Trans. Soc. Rheol. **18**, 247-269 (1974).
12. P. Dantu, *Annales des Ponts et Chaussées*, n° 4 (1967).
13. C.T. Veje, Master's thesis, University of Copenhagen (1995).
14. W.A. Beverloo, H.A. Leniger, J. Van De Velde, Chem. Engng. Sci. **15**, 260 (1961).
15. R.L. Brown, Nature **191**, 458 (1961).
16. T. Le Pennec *et al.*, preprint (1998).